SOLID-SOLID BONDING CHARACTERIZATION BY ULTRASONIC REFLECTIVITY

Tran D. K. Ngoc, Herbert J. Ruf and Kin W. Ng

Department of Physics
Georgetown University
Washington, DC 20057

INTRODUCTION

The most common approach to model a weakened bond at a solid-solid interface has been to allow for a partial slip of the displacement at the interface. This concept is transformed into a specific set of boundary conditions which are then solved to obtain the plane-wave reflection and transmission coefficients or to determine the dispersion relation of the associated interface wave, if they exist. A key question in this approach is whether one allows for a partial slip in both displacement components or just the tangential. Initially, Murty [1-2] considered only the tangential slip to model the slip interface with the following boundary conditions:

- Normal stress is continuous,
- Shear stress is continuous,
- Normal displacement is continuous, and
- Shear stress is proportional to a tangential displacement slip.

Using this set of boundary conditions, Murty derived a dispersion relation to investigate the existence of the interface wave propagating along such a slip interface [1]. He also investigated the reflection and transmission of a compressional incident wave for several representative solid-solid combinations [2]. More generally, the boundary conditions at a slip interface were formulated by Schoenberg [3] in the form of a 3X3 boundary stiffness matrix, which has two independent elements, normal stiffness k_N and tangential stiffness k_T. Schoenberg's formulation provides a rigorous basis to treat a slip interface, but his numerical results are mostly concerned with the special case of normal incidence. This general approach was also used by Pilarski [4-6], who formulated the boundary conditions in a fashion similar to Murty's, with the exception that the normal stress is proportional to a normal displacement slip.

In most works reported to date, the reflection coefficients were computed numerically from the set of linear equations representing the boundary conditions. In this paper, the explicit expressions for the reflection coefficients will be derived for both shear and compressional incidences. The analytical results will then be used to compute the reflection amplitude for a metal-metal interface. Computational

predictions will be analyzed to arrive at a conceptual inspection technique for estimating the bonding strength at the considered interfaces.

THEORY

In the x-z plane, consider two elastic half-spaces joined at z=0 under the slip-interface conditions. First, let the incident wave be compressional in the upper half-space z>0. The formal solutions of the displacement potentials φ (compressional) and Φ (shear) in the two halfspaces for such a problem are:

For z>0:

$$\varphi = P_i\exp(ikpz) + P_r\exp(-ikpz),$$
$$\Phi = S_r\exp(-ikqz), \tag{1}$$

For z<0:

$$\varphi' = P_t\exp(ikp'z),$$
$$\Phi' = S_t\exp(ikq'z), \tag{2}$$

in which the harmonic term exp[ik(ct-x)] is suppressed for brevity. In Eqs.(1-2), k and c are the wave number and phase velocity in the x direction; P_i, P_r, S_r, P_t, and S_t are constants to be determined by the boundary conditions at z=0; and p, p', q, and q' are defined by

$$p = [(c^2/\alpha^2)-1]^{\frac{1}{2}},$$
$$q = [(c^2/\beta^2)-1]^{\frac{1}{2}},$$
$$p' = [(c^2/\alpha'^2)-1]^{\frac{1}{2}}, \tag{3}$$
$$q' = [(c^2/\beta'^2)-1]^{\frac{1}{2}},$$

where α, β, α', and β' are the compressional and shear sound velocities in the upper and lower half-spaces, respectively. Throughout this paper, the primed variables are used to denote the same physical quantities in the lower half-space.

In practice, we believe that use of the tangential slip alone is more than adequate to model a weakened bond, therefore, the boundary conditions employed by Murty are used to describe a slip interface. According to Murty [1], the tangential stiffness k_T can be expressed in the form

$$k_T = (i\delta\beta^2 kc/\alpha)[B/(1-B)], \tag{4}$$

where B is a normalized bonding parameter, ranging from 0 to 1. When k_T=B=0, there is no bonding between the two solids; when B=1 or $k_T=\infty$, the bonding is perfect. Note that in Eq.(4), δ is the density of the upper solid.

Expressing the displacement and stress components in terms of the displacemnt potential φ and Φ, one can apply the boundary conditions to obtain the following matrix equation:

$$\begin{bmatrix} 2bp+\frac{B}{\sin\Theta_i} & br-\frac{Bq}{\sin\Theta_i} & \frac{-B}{\sin\Theta_i} & \frac{Bq'}{\sin\Theta_i} \\ p & 1 & p' & -1 \\ -mr & 2mq & r' & 2q' \\ 2mp & mr & 2p' & -r' \end{bmatrix} \begin{bmatrix} R_{pp} \\ R_{ps} \\ T_{pp} \\ T_{ps} \end{bmatrix} = \begin{bmatrix} 2bp-\frac{B}{\sin\Theta_i} \\ p \\ mr \\ 2mp \end{bmatrix} \tag{5}$$

where $b = 1-B$, $m = \mu/\mu'$ and $r = 1-q^2$.

In the case of shear incidence, the above algebraic steps can be repeated, starting from the following formal solutions:

For $z>0$:

$$\varphi = P_r\exp(-ikpz),$$
$$\Phi = S_i\exp(ikqz) + S_r\exp(-ikqz), \tag{6}$$

For $z<0$:

$$\varphi' = P_t\exp(ikp'z),$$
$$\Phi' = S_t\exp(ikq'z). \tag{7}$$

Application of the boundary conditions leads to a matrix equation similar to Eq.(5):

$$\begin{bmatrix} 2bp+\frac{B}{\sin\Theta_i} & br-\frac{Bq}{\sin\Theta_i} & \frac{-B}{\sin\Theta_i} & \frac{-Bq'}{\sin\Theta_i} \\ p & 1 & p' & -1 \\ -mr & 2mq & r' & 2q' \\ 2mp & mr & 2p' & -r' \end{bmatrix} \begin{bmatrix} R_{sp} \\ R_{ss} \\ T_{sp} \\ T_{ss} \end{bmatrix} = \begin{bmatrix} -br-\frac{Bq}{\sin\Theta_i} \\ -1 \\ 2mq \\ -r \end{bmatrix} \tag{8}$$

The explicit expressions of the four reflection coefficients for two types of incidence can be obtained from Eqs.(5,8). For example, the reflection coefficient R_{PP}, i.e. compressional incidence and compressional reflection, was found to be:

$$R_{PP} = (N_{PP}/D), \tag{9}$$

where

$$\begin{aligned} N_{PP} &= (1-B)[p(r-2)(4p'q'+r'^2)+mp'(r'-2)(4pq-r^2)] \\ &\quad + \frac{B}{\sin\Theta_i}\{m[2(2p'q'+r')(2pq-r)-(r'-2)(r-2)(pq'-p'q)] \\ &\quad -(pq-1)(r'^2+4p'q')-m^2(p'q'+1)(4pq-r^2)\}, \\ D &= (1-B)[p(r-2)(4p'q'+r'^2)+mp'(r'-2)(4pq+r^2)] \\ &\quad + \frac{B}{\sin\Theta_i}\{m[2(2p'q'+r')(2pq+r)-(r'-2)(r-2)(pq'+p'q)] \\ &\quad -(pq+1)(r'^2+4p'q')-m^2(p'q'+1)(4pq+r^2)\}. \end{aligned} \tag{10}$$

Note that the numerators of the various coefficients are different, while the denominator D, which when set equal to zero yields the dispersion relation of the interface wave, remains the same for all coefficients. The numerators of the other reflection coefficients are:

$$
\begin{aligned}
N_{PS} &= (1-B)4mpp'r(r'-2) \\
&\quad + \frac{2Bp}{\sin\Theta_i}[m(r+2)(r'+2p'q')-(r'^2+4p'q')-2m^2r(1+p'q')], \\
N_{SP} &= (1-B)[r^2(1-m)(r'+2p'q')-4mr(r'-2)p'q] \\
&\quad + \frac{B}{\sin\Theta_i}\{2q[(r'-r)(r'+2p'q')-2(r'-2)p'(q'-mq)] \\
&\qquad +(1+p'q')[2(1-m)r(q'-mq)-4m(r'-r)q]\}, \\
N_{SS} &= (1-B)\{2p[(r'-r)(r'+2p'q')-2(r-2)p(q'-mq)] \\
&\qquad +r[(2m-r')p(r'+2p'q')-p'(r-2)(mr-2pq')]\} \\
&\quad + \frac{B}{\sin\Theta_i}\{(1-pq')[(r'-r)(r'+2p'q')-2(r-2)p(q'-mq)] \\
&\qquad +(q'-q)[p'(r-2)(mr-2pq')-p(2m-r')(r'+2p'q')] \\
&\qquad +(1+p'q')[(r'-r)(2pq'-mr)-2p(2m-r')(mq-q')]\}.
\end{aligned}
\tag{11}
$$

COMPUTATIONAL RESULTS

The previous theoretical results have been applied to several systems. These systems can be broken into two groups, those in which the interface is between identical solids and those in which the interface is between different solids. The identical solid systems make use of three materials: Aluminum, Brass and Silicon Carbide while the different solid system consists of the Aluminum-Brass interface. The following parameters were used in the calculations:

	Compressional Velocity (Km/s)	Shear Velocity (Km/s)	Density (g/cm^3)
SiC	11.67	7.47	3.08
Al	6.32	3.13	2.70
Brass	4.28	2.03	8.56

Figures 1a-1c are plots of reflectivity versus incident angle for the identical solid systems. The four curves on each represent different modes of propagation, before and after reflection, the s representing shear and the p representing compressional. For example the sp curve is the reflectivity of a shear incident wave into a compressional reflected wave.

Note that the general features of the various curves, for a given mode, are similar in all three sets of curves. The ss curves have a peak near normal incidence and then fall to minimum reflectivity at higher angles. The pp curves are just the reverse, rising from a minimum at near normal incidence to a well defined peak at higher angles. The sp curves tend to rise from a minimum at 0° to a maximum at 90°; while the ps curves have broad, less well defined peaks in the middle angles.

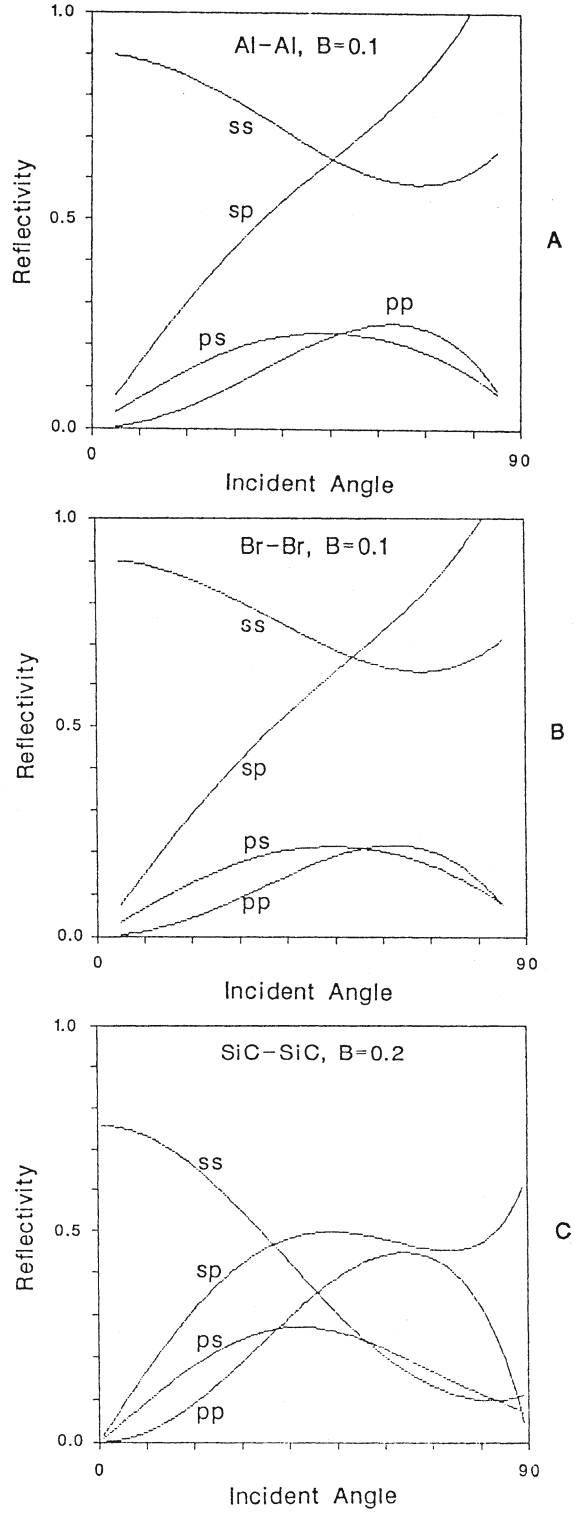

Fig. 1. Reflectivity versus incident angle for three systems of identical solids (a) Aluminum-Aluminum, (b) Brass-Brass, and (c) Silicon Carbide-Silicon Carbide.

In terms of modes that would be more useful for practical purposes, we believe that the ss and pp should be chosen. The reasons for this are: (1) the sp and ps modes are more difficult to excite and observe; (2) their angular dependence varies more with different materials; and (3) the ss and the pp modes have peak reflectivities at angles which are accessible, but well separated from each other, resulting in less difficulty in interpretation of the data.

Figure 2 is a plot of reflectivity versus incident angle in the Al-Al system, for various values of B. Here we see that the sensitivity of the ss curves, to changes in B, is approximately the same over the full range of angles. Therefore the optimal angular region for making measurements with the ss mode is where the reflectivity is largest, near normal incidence. The pp curves on the other hand exhibit useful reflectivity and sensitivity to changes in B in a narrower range of angles centered around 60°. Figure 3 is a plot of the reflectivity versus B for incident angles in these two regions.

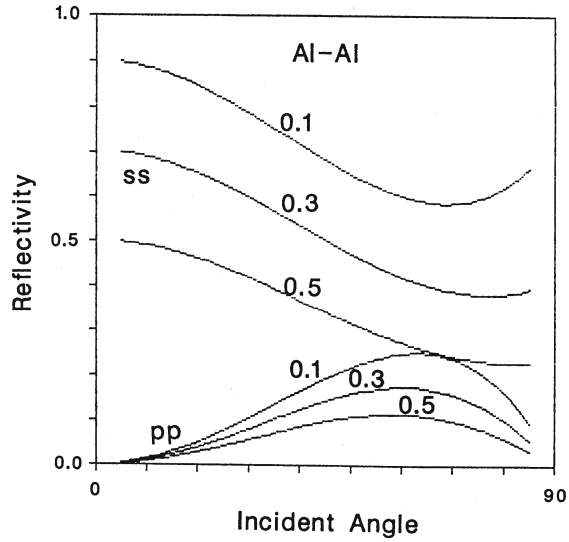

Fig. 2. Reflectivity versus incident angle in the Al-Al system, for various values of B.

We see that the variation of reflectivity with B is nearly linear in both cases, with a steeper slope for the ss mode. Either of these curves would be useful for determining the bonding parameter of the Al-Al system, with the ss mode yielding better resolution.

We now turn to systems with different solids on either side of the interface. The system studied is the Aluminum-Brass interface. Figures 4a and 4b are plots of reflectivity versus incident angle, similar to figure 1.

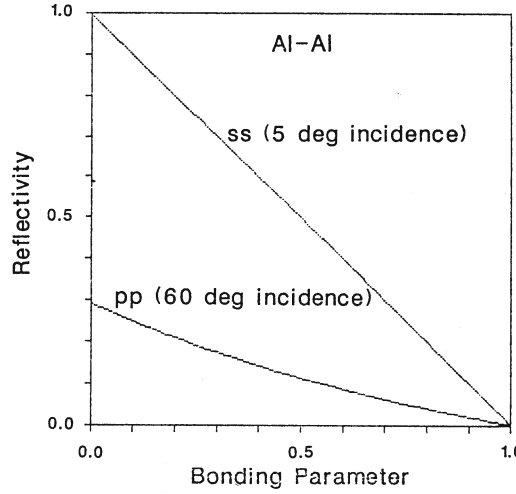

Fig. 3. Reflectivity versus B for the Al-Al system.

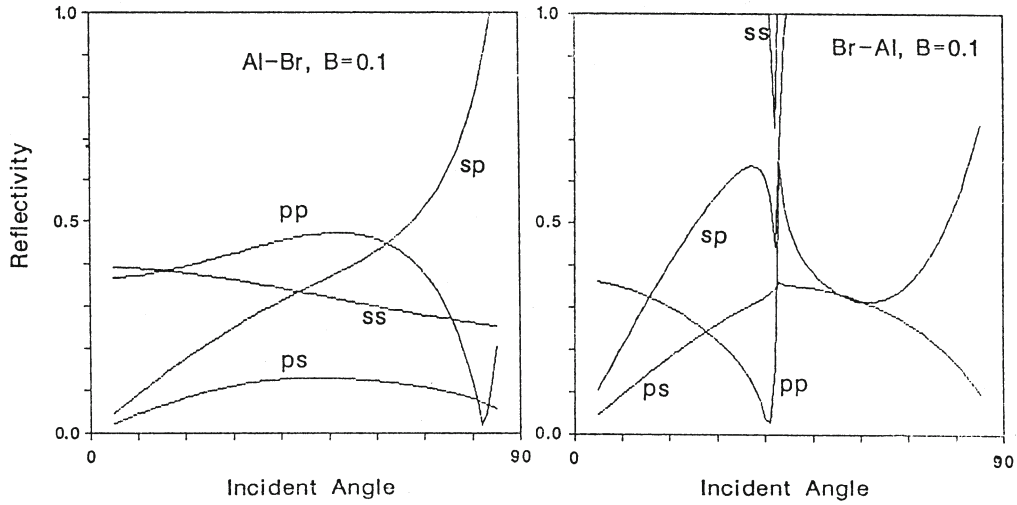

Fig. 4. Reflectivity versus incident angle for the Aluminum-Brass system with (a) Aluminum as the incident solid, and (b) Brass as the incident solid.

It is immediately apparent that the situation is now more complex than it was previously. Figure 4a presents an interface with Aluminum as the incident solid, i.e. the solid containing the incident and reflected beams, while figure 4b has brass as the incident solid. Note that the curves in 4a are similar to the respective curves in figure 1, while those in 4b display a discontinuity around 40°. This discontinuity is associated with the existence of an interface wave mode. Due to the complexity of the curves it would be very difficult to interpret data taken with brass as the incident solid. For this reason we would choose to do interface characterization with Aluminum as the incident solid.

Figure 5 is a plot of the reflectivity versus B for such a system, where we have chosen to look at the pp and ss modes for similar reasons to those given previously. In this plot note that the pp mode is approximately a linear function of B, with good enough sensitivity to changes in B to be useful. The ss curve on the other hand, while linear

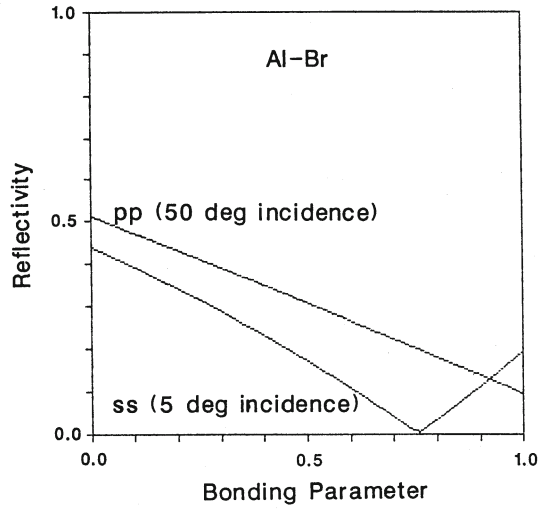

Fig. 5. Reflectivity versus B for the Al-Brass system with Al as the incident solid.

in B, exhibits a slope change at around B=.75. This results in a situation where for values of B greater than approximately 0.5, two values of B correspond to the same reflectivity. This limits the usefulness of the ss mode to values of B less than 0.5.

CONCLUSIONS

In the reported research, a weakened bond at a solid-solid interface was modeled by allowing for a partial slip in the tangential displacement component. Explicit expressions of the reflection coefficients were derived for both compressional and shear incidences. The computational results suggested that the reflection amplitude can be used to estimate the bonding strength at such an interface. Application of this theoretical model to the Al-Al, Brass-Brass and SiC-SiC joints recommends that it is optimal to characterize an Al-Al joint by using a 5° shear beam or a 60° compressional beam. For an Al-Brass joint, it is probably more advantageous to interrogate the bond line with incidence from the Al halfspace.

REFERENCES

1. G.S. Murty, "A Theoretical Model for the Attenuation and Dispersion of Stoneley Waves at the Loosely Bonded Interface of Elastic Half Spaces," Physics of the Earth and Planetary Interiors **11**, 65 (1975).
2. G.S. Murty, "Reflection, Transmission and Attenuation of Elastic Waves at a Loosely Bonded Interface of Two Half Spaces," Geophys. J. R. Astr. Soc. **44**, 389 (1976).
3. M. Schoenberg, "Elastic Wave Behavior across Linear Slip Interfaces," J. Acoust. Soc. Am. **68**, 1516 (1980).
4. A. Pilarski, "The Coefficient of Reflection of Ultrasonic Waves from An Adhesive Bond Interface," Archives of Acoustics **8(1)**, 41 (1983).
5. A. Pilarski, "Ultrasonic Evaluation of the Adhesion Degree in Layered Joints," Materials Evaluation **43**, 765 (1985).
6. A. Pilarski, "Leaking Interface Waves in Ultrasonic NDE," Proc. 11th World Conf. NDT, Las Vegas (1985).